Desalination and Water Treatment
www.deswater.com
doi: 10.1080/19443994.2013.810325

52 (2014) 4990–4998
July

Taylor & Francis
Taylor & Francis Group

Bio-Fenton process for Acid Blue 113 textile azo dye decolorization: characteristics and neural network modeling

Mohammadreza Eskandarian[a,b,*], Fatemeh Mahdizadeh[c], Leila Ghalamchi[b], Saber Naghavi[d]

[a]*Faculty of Chemistry, Department of Applied Chemistry, University of Semnan, Semnan, Iran*
Tel. +98 9123415643; Fax: +98 4113340191; email: m.r.eskandarian@gmail.com
[b]*Faculty of Sciences, Water & Wastewater Treatment Research Laboratory, Department of Chemistry, University of Zanjan, Zanjan, Iran*
[c]*Faculty of Chemistry, Department of Applied Chemistry, University of Tabriz, Tabriz, Iran*
[d]*Faculty of Sciences, Department of Chemistry, Islamic Azad University, Karaj, Iran*

Received 26 July 2012; Accepted 7 May 2013

ABSTRACT

In this study, decolorization of Acid Blue 113 textile azo dye (AB 113) by a bio-Fenton process has been performed in an aqueous medium. The bio-Fenton oxidation process tested is the oxidation process of glucose for H_2O_2 generation and *in situ* use of H_2O_2 with Fe^{2+} as Fenton reagents to produce hydroxyl radicals which degrade the organic dyes. The effect of different parameters such as AB 113, glucose, $FeSO_4$ concentrations, and also the glucose oxidase activity on the decolorization of AB 113 dye was assessed. Artificial neural network was used to simulate the decolorization of AB 113 aqueous solution. Different networks were designed for this process. The best network was 5-14-1 due to the best coefficient of determination (0.996) and mean square error (0.42). The results indicated that ANN is provided reasonable predictive performance.

Keywords: Acid Blue 113; Artificial neural network; Bio-Fenton; Decolorization; Glucose oxidase

1. Introduction

Synthetic dyes vastly are used in many industries such as textile, leather, plastic, paper, cosmetics, print, pharmaceutical, and food industries. They are major sources of environmental, especially water, pollution [1]. Releases of the wastewater of these industries to environment without treatment are damageable and retrievable. Existence of chromatic materials in water reduces the influence of light and photosynthesis of aquatic plants. Toxicity of dyes caused death of aquatic life forms [2]. An additional difficulty is that these dyes are not easily degraded by common wastewater treatment systems. Therefore, the employment of these dyes must be managed and must be treated before being released into the environment [3].

Numerous processes such as ozonation, photooxidation, flocculation and coagulation, adsorption, froth flotation, reverse osmosis, ion exchange, and membrane filtration have been tested for color removal [4]. Nevertheless, expensive plant requirements,

*Corresponding author.

high-operational costs, regeneration problem, secondary pollutants, sensitivity to variations in wastewater input, interference by other wastewater constituents, and residual sludge generation are some technological and economical disadvantages of these methods [5,6].

Azo dyes, the largest class of synthetic dyes, are characterized by structures with one or more azo group (–N=N–) that are bounded to the aromatic rings. It has to be emphasized that due to their complicated and recalcitrant molecular structure, they are difficult to remove from wastewater by using common physical, chemical, and biological treatment methods [7,8]. Therefore, it is essential to look for appropriate methods or techniques for the treatment of this kind of pollutants to reduce their environmental impact.

Currently, the major methods of textile wastewater treatment are advanced oxidation processes [9] which include bleaching, ozonation, Fenton oxidation [10], and wet-air oxidation. Fenton reagent exhibits a number of features that make its use advantageous as compared to other methods such as high catalytic efficiency, high specificity, absence of side reactions, and cost-effectiveness. Experimental observations indicate that it can be used to degrade many pesticides [11], harmful chemicals [12], dyes [13], etc.

Hydroxyl radicals have great oxidizing potential ($E^o = 2.8$ V), so they can quickly and non-selectively oxidize a wide diversity of organic dyes [14]. So, advanced oxidation processes can be a good selection to treat this kind of wastewaters because of their powerful oxidizing capability to oxidize dyes to nontoxic products of CO_2 and H_2O [15]. This method does not have the problem of residuals and also can be used in room temperature and atmospheric pressure [16]. In Fenton process, ferrous ion reacts with hydrogen peroxide to produce hydroxyl radical as Eq. (1) [2]:

$$Fe^{2+} + H_2O_2 \longrightarrow Fe^{3+} + HO^{\bullet} + HO^{-} \quad (1)$$

Bio-Fenton process includes H_2O_2 production through the glucose oxidation in the presence of glucose oxidase (GOx) as the biocatalyst and *in situ* consumption of generated H_2O_2 for reacting with Fe^{2+} to generate hydroxyl radicals which degrade the organic dyes [17].

For the present investigation, water soluble disazo dye Acid Blue 113 (Molecular formula: $C_{32}H_{21}N_5Na_2O_6S_2$ and molecular weight of 681.65 g/mol) (Sigma-Aldrich) was selected. AB113 is toxic and carcinogenic in nature (LD50 > 2,000 mg/kg and LC50 1–10 mg/l). In this study, we considered a neural network modeling for bio-Fenton process of AB113 azo dye degradation. In this study, the optimal condition of bio-Fenton reaction was investigated. An artificial neural network, which consists of many simple process units, can simulate the structural organization and function of a human brain. The usage of artificial neural network (ANN) has several advantages, some of them being listed below [18].

(1) ANN estimates reaction rate without requiring any kinetic model equation.
(2) Estimation of reaction rate without a kinetic model eliminates the errors arising from the selection of kinetic model, and the estimation of kinetic constants.
(3) Usage of ANN reduces the number of the experimental work and provides more information.

ANN was used for simulation and modeling of AB 113 removal from water by enzymatic method and the best structure of neural network for this process was determined.

2. Materials and methods

2.1. Chemicals and reagents

GOx type II (EC 1.1.3.4, 25 U/mg, from *Aspergillusniger*-solid, molecular weight: 160 kDA), β-D-(+)-glucose ($C_6H_{12}O_6$)/molecular weight: 180.16 g mol^{-1}, sodium acetate ($C_2H_3NaO_2$)/molecular weight: 82.03 g mol^{-1}, acetic acid ($C_2H_4O_2$)/molecular weight: 60.05 g mol^{-1}, sulfuric acid (H_2SO_4)/molecular weight: 98.08 g mol^{-1}, sodium hydroxide (NaOH)/molecular weight: 40 g mol^{-1}/ solid, 2,2´-azino-di-[3-ethylbenzthiazolin-sulfonate]/(formula: $C_{18}H_{16}N_4O_6S_4$)/molecular weight: 514.6 g mol^{-1}/solid, $FeSO_4$ (molecular weight: 151.91)/ solid, and Acid Blue 113 (AB 113)/ (molecular formula: $C_{32}H_{21}N_5Na_2O_6S_2$/molecular weight: 681.65 g mol^{-1}/λ_{max} = 566 nm/soluble in water) in the analytical grade were obtained from Sigma Aldrich Corporation.

All reagents are of analytical purity. There were made some pH adjustments during the bio-Fenton process or final treatment corrections using some common acid and alkaline solutions (H_2SO_4 0.1 M and/or NaOH 0.1 M) and also buffer solution (sodium acetate).

2.2. Analytical methods

The absorption spectrum of AB 113 in aqueous solution was recorded in the range of 400–850 nm, and it was found that the maximum wavelength was at 566 nm. Aqueous solutions of AB 113 with different concentrations were prepared, and their absorption at

566 nm was measured and calibration curve, for finding dye concentration in decolorization experiments, was plotted.

The concentration of AB 113 at different reaction times was determined by measuring the absorption intensity of the solution at 566 nm. The decolorization efficiency of AB 113 is defined as follows [1]:

$$R(\%) = \frac{C_0 - C_t}{C_0} \times 100 \quad (2)$$

where R is decolorization efficiency, C_0 is initial AB113 concentration, and C_t is AB113 concentration at t, min.

UV–Vis spectrophotometer made in England Biowave S2100-WPA was used for absorption measurements, related to a blank with distillate water.

2.3. Experimental procedures

All experiments were carried out in a 100 mL flask bioreactor in a shaker incubator at 160 rpm. We used five parallel samples in order to get comparison of all performed experimental results. Temperature of the reaction mixture in all experiments was constant at 23 ± 1 ℃. The initial pH of solutions was adjusted by using acetate buffer (0.1 M), 0.1 mol/L sulfuric acid, and 0.1 mol/L sodium hydroxide solutions by pH meter Labtron (PHT-110). The required concentrations of glucose, glucose oxidase, $FeSO_4$, and AB 113 were prepared in deionized water correspondingly.

As can be seen from Eq. (3), the production rate of H_2O_2 depends on glucose concentration. Due to this reason, the effect of glucose concentration on the decolorization of AB 113 was examined in different initial concentration of glucose from 0.005 to 0.05 mol/L, while concentration of dye (40 mg/L), Fe^{2+} (0.2 mmol/L), GOx activity (2,000 U/L), and the initial pH (4.0) were constant.

A series of experiments were performed with different initial Fe^{2+} concentrations (0.1, 0.15, 0.2, 0.25, 0.3, 0.35, 0.4 mmol/L) for studying the effect on dye removal while the concentration of dye (40 mg/L), glucose (0.02 mol/L), GOx activity (2,000 U/L), and initial pH (4.0) were constant.

The effect of initial pH on the decolorization of AB 113 by bio-Fenton process has been shown in Fig. 2(d). The experiments were done at constant concentration of dye (40 mg/L), glucose (0.02 mol/L), Fe^{2+} (0.2 mmol/L), and initial GOx activity (2,000 U/L) while the pH varied from 3.0 to 7.0 with 0.5 interval of variation. The pH 3.0 and 4.0 were adjusted with H_2SO_4 and sodium hydroxide solutions (1.0 M), and pH 5.0–7.0 was adjusted with acetate buffer solution.

2.4. GOx activity determination

GOx oxidizes β-D-glucose in the presence of oxygen to β-D-glucono-δ-lactone and H_2O_2. The produced H_2O_2 is then utilized to oxidize a chromogenic substrate in a secondary reaction in the presence of catalase and a resultant color change is monitored spectrophotometrically. 2,2′-Azino-di-[3-ethylbenzthiazolin-sulfonate] was used for forming a greenish-blue oxidized product that was measured spectrophotometrically at 420 nm. One unit of catalyst activity (U) is defined as the amount of GOx required to consume 1 μmol substrate in one min at 25℃ [19].

2.5. Construction of ANN model

The ANN was used to model AB 113 decolorization from solution that was created by writing computer codes in Matlab 7.1. The enzymatic AB 113 decolorization was modeled using five variables as the input parameters of the network: pH, dye concentration, Fe^{2+} concentration, glucose concentration, and GOx activity while temperature and shaking rate were constant. Percentage of AB 113 decolorization after 60 min was used as the output parameter.

3. Results and discussion

3.1. Bio-Fenton process

Water soluble bisazo dye Acid Blue 113 (Fig. 1) was selected for degradation by Bio-Fenton reaction [20].

Total bio-Fenton reaction used is:

$$C_6H_{12}O_6 + H_2O + O_2 \xrightarrow{\text{Glucoseoxidase}} C_6H_{12}O_7 + H_2O_2 \quad (3)$$

$$M^{n+} + H_2O_2 \longrightarrow M^{(n+1)+} + HO^- + OH\bullet \quad (4)$$

where M is a transition metal like iron [18].

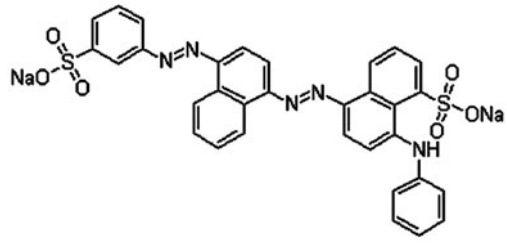

Fig. 1. Molecular structure of Acid Blue 113 [21].

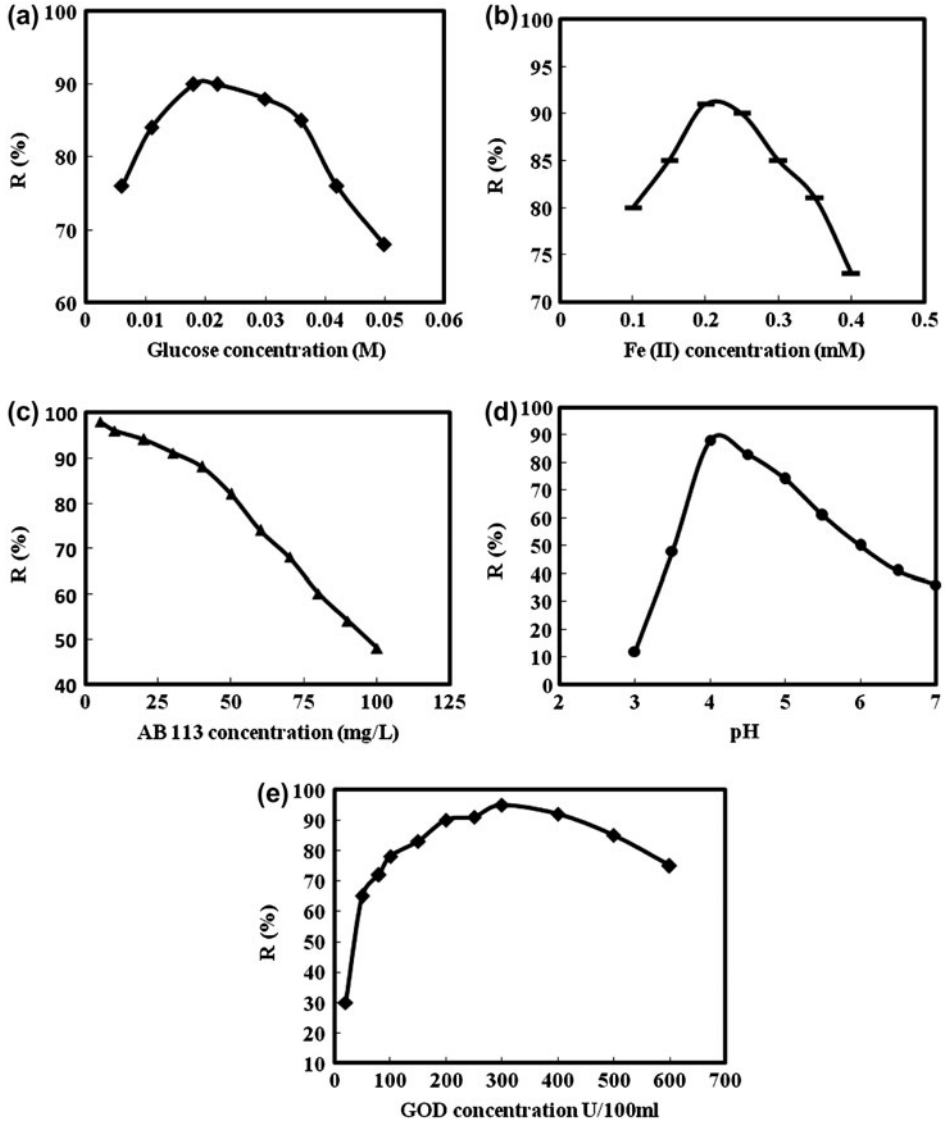

Fig. 2. Investigation of the effect of each variable on percentage of AB 113 decolorization by Bio-Fenton process. (a) Glucose concentration, (b) Fe^{2+} concentration, (c) AB 113 concentration, (d) pH, and (e) GOx activity.

3.2. Comparison of AB 113 absorption spectrum with other material

For determination of the efficiency and rate of decolorization, dye concentration measuring in different steps is necessary. For awareness of uninterference of the spectrum peaks of AB 113 with $FeSO_4$, glucose, and GOx, their absorption spectrum were recorded in the range of 400–800 nm. Effect of initial AB 113 concentration on decolorization process was tested using different concentrations of AB 113 (5, 10, 20, 30, 40, 50, 60, 70, 80, 90, 100 mg/L), while glucose concentration (0.02 mol/L), Fe^{2+} concentration (0.2 mmol/L), initial GOx activity (2,000 U/L), and the pH (4.0) were constant. Comparison of the results indicates that AB 113 has spectrum peak at 566 nm. So, AB 113 concentration easily can be calculated spectrophotometrically.

3.3. Effect of glucose concentration

Dye decolorization efficiency in each concentration of glucose after 60 min is shown in Fig. 2(a); from the figure, it can be observed that increasing the glucose concentration from 0.005 to 0.02 mol/L has caused increasing in the decolorization of AB 113. However, further increase of the glucose concentration above 0.02 mol/L had negative effect on the decolorization rate of AB 113. Because in the high concentrations of glucose, there is the scavenging effect of excessive

produced H_2O_2 to •OH [Eqs. (5)–(7)]. Also, with the recombination of hydroxyl radicals [Eq. (8)], amounts of •OH were declined and following it, the decolorization efficiency of AB 113 was reduced [7,21].

$$H_2O_2 + OH^{\cdot} \longrightarrow HO_2^{\cdot} + H_2O \quad (5)$$

$$H_2O_2 + OH_2^{\cdot} \longrightarrow HO^{\cdot} + O_2 + H_2O \quad (6)$$

$$OH^{\cdot} + OH_2^{\cdot} \longrightarrow O_2 + H_2O \quad (7)$$

$$HO^{\cdot} + HO^{\cdot} \longrightarrow H_2O_2 \quad (8)$$

3.4. Effect of the initial Fe^{2+} concentration

The lowest and the highest degradation efficiency were obtained at initial Fe^{2+} concentration of 0.1 and 0.2 mmol/L, respectively, after 60 min of reaction time. The results have been presented in Fig. 2(b). The degradation efficiency of AB 113 was significantly changed over the initial Fe^{2+} concentration value of 0.1–0.4 mmol/L.

Concentration of 0.25 mmol/L $FeSO_4$ has no increasing effect in AB 113 degradation efficiency. Much higher concentration of Fe^{2+} (0.4 mmol/L) leads to excessive •OH value and self-scavenging of •OH radical by Fe^{2+} (Eq. (9)) that causes the decreasing in decolorization rate of AB 113 [3].

$$Fe^{2+} + HO^{\cdot} \longrightarrow Fe^{3+} + HO^{-} \quad (9)$$

3.5. Effect of initial AB 113 concentration

The results are shown in Fig. 2(c). It is observed that in the lower concentrations of the dye, decolorization is faster. The high concentration of dye in aqueous solution increases the number of dye molecules in the solution while the number of hydroxyl radicals is constant [22]; so despite of the increase of color removal rate, the decolorizing efficiency decreases at high concentrations of dye.

3.6. Effect of initial pH

The optimum pH was observed at 4.0. Increasing or decreasing of the pH value of dye solution had undesirable effects on the decolorization rate of AB 113. This is because of the concentrations of Fe^{2+} and H_2O_2 depend on pH, and, correspondingly, pH affects on the yield of active •OH and decolorization rate. The decolorization efficiency of AB 113 was decreased with the increase of pH from 4.0 to 7.0. This is mainly caused by the fact that $Fe(OH)_3$ is formed when pH is high [1], and inhibit the reaction between Fe^{2+} and H_2O_2. Therefore, only a small amount of the •OH is generated. When the pH is lower than 4.0 approximately, GOx is become inactive and just a little amount of H_2O_2 is produced [23]. Thus, the rate and the efficiency of AB 113 degradation are decreased, correspondingly. In addition, when the pH of reaction environment is lower than 3.0, H_2O_2 reacts with excessive H^+ and forms oxonium ion (H_3O^+) [4] which do not have positive role on the decolorization.

3.7. Effect of GOx concentration

As shown in Fig. 2(e), the dye degradation rate increases with increasing GOx activity until to 3,000 U/L. In the presence of high GOx activity, due to high rate of H_2O_2 production, reaction between active radicals and produced H_2O_2 is done, and this reaction decreases the AB 113 degradation rate [24].

3.8. Modeling by ANN

3.8.1. The number of neurons and hidden layers

It is important to find a right structural organization of neural network. In fact, the number of neurons and the hidden layers of network are chosen by experience, because no uniform method has been developed to decide it yet in theory [25]. By trying in time, a better structural organization of network could be found; the result is listed in Fig. 3. Different neural networks were designed with one hidden layer and different number of neurons in it.

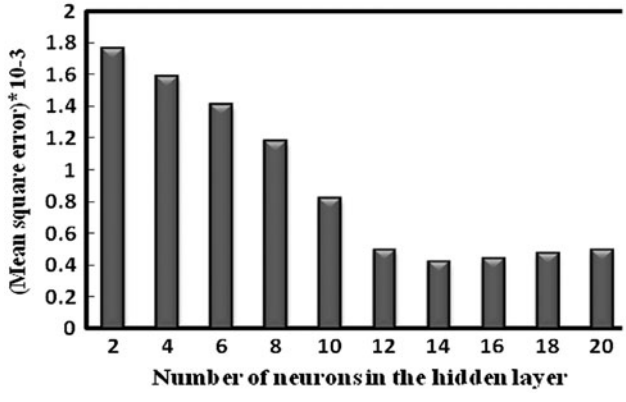

Fig. 3. Effect of the number of neurons in the hidden layer on the performance of the neural network (MSE).

Table 1
List of experiments were used for training and testing of neural networks

No.	Dye C_0 (mg/L)	Fe^{2+} C_0 (mM)	Glucose C_0 (mM)	GOx activity U/L	pH	Experimental dye removal efficiency	Predicted dye removal efficiency
1	50	0.2	0.006	1,500	3.8	68	66.18
2	50	0.2	0.011	1,500	3.8	80	79.15
3	50	0.2	0.018	1,500	3.8	85	86.73
4	50	0.2	0.022	1,500	3.8	86	85.38
5	50	0.2	0.03	1,500	3.8	84	84.2
6	50	0.2	0.036	1,500	3.8	81	80.75
7	50	0.2	0.042	1,500	3.8	72	71
8	50	0.2	0.05	1,500	3.8	64	63
9	40	0.1	0.018	2,000	4	79	83.5
10	40	0.15	0.018	2,000	4	87	90.2
11	40	0.2	0.018	2,000	4	92	91.7
12	40	0.25	0.018	2,000	4	91	91.05
13	40	0.3	0.018	2,000	4	89	89.16
14	40	0.35	0.018	2,000	4	81	81.14
15	40	0.4	0.018	2,000	4	77	86.93
16	5	0.18	0.02	2,500	4.2	92	92.86
17	10	0.18	0.02	2,500	4.2	89	89.47
18	20	0.18	0.02	2,500	4.2	85	85.8
19	30	0.18	0.02	2,500	4.2	78	77.85
20	40	0.18	0.02	2,500	4.2	72	72.23
21	50	0.18	0.02	2,500	4.2	68	68.42
22	60	0.18	0.02	2,500	4.2	64	64.69
23	70	0.18	0.02	2,000	4	59	59.85
24	80	0.18	0.02	2,000	4	54	53.59
25	90	0.18	0.02	2,000	4	50	50.32
26	100	0.18	0.02	2,000	4	47	47.09
27	40	0.2	0.018	2,000	3	10	10.8
28	40	0.2	0.018	2,000	3.5	44	44.91
29	40	0.2	0.018	2,000	4	80	79.86
30	40	0.2	0.018	2,000	4.5	78	79.5
31	40	0.2	0.018	2,000	5	70	69.55
32	40	0.2	0.018	2,000	5.5	57	57.26
33	40	0.2	0.018	2,000	6	46	47
34	40	0.2	0.018	2,000	6.5	37	37.8
35	40	0.2	0.018	2,000	7	32	32.15
36	50	0.2	0.006	1,500	3.8	68	66.18
Validation data							
37	35	0.22	0.025	200	4	26	26.5
38	35	0.22	0.025	500	4	61	60.88
39	35	0.22	0.025	800	4	68	67.95
40	35	0.22	0.025	1,000	4	74	74.2
41	35	0.22	0.025	1,500	4	79	79.22
42	35	0.22	0.025	2,000	4	84	84.09
43	35	0.22	0.025	2,500	4	87	87.23
44	35	0.22	0.025	3,000	4	91	90.86
45	35	0.22	0.025	4,000	4	88	87.23
46	35	0.22	0.025	5,000	4	81	80.41

(*Continued*)

Table 1
(*Continued*)

No.	Dye C_0 (mg/L)	Fe^{2+} C_0 (mM)	Glucose C_0 (mM)	GOx activity U/L	pH	Experimental dye removal efficiency	Predicted dye removal efficiency
Testing data							
47	35	0.22	0.025	6,000	4	71	69.7
48	30	0.2	0.006	1,500	3.5	69	69.11
49	30	0.2	0.011	1,500	3.5	77	77.27
50	80	0.2	0.018	3,000	3.5	65	65.59
51	90	0.2	0.018	3,000	3.5	60	59.35
52	100	0.2	0.018	3,000	3.5	56	55.45
53	20	0.2	0.018	200	4	26	26.35
54	20	0.2	0.018	500	4	61	59
55	60	0.2	0.018	800	4	68	69.03
56	60	0.2	0.018	1,000	4	74	73.09

3.8.2. Training and testing of artificial neural network

Before training, normalization was applied on the input and output data (X) to calculate the normalized input and output values (X^*) using Eq. (3) [26]:

$$X^* = \frac{X - \min(X)}{\max(X) - \min(X)} \tag{10}$$

The back propagation algorithm was constructed as the learning algorithm to adapt the weights. Tansig and purlin were selected as transfer and training function, respectively. Thirty-six data were used for training of the ANN, 10 data were used as testing, and 10 data were applied as validating the trained network (Table 1). The training data-set (five input and their corresponding desired responses) was presented to the network, and a feedforward algorithm automatically adjusted the weights. This means that the artificial neurons are organized in layers, and send their signals "forward", and then the errors are propagated backwards. The network receives inputs by neurons in the input layer, and the output of the network is given by the neurons on an output layer [27]. Estimation was made and the results were compared with the corresponding experimental value. Then the estimation error (the difference between the estimated and the experimental values) was distributed across the network in a manner which allowed the interconnection weights to be modified according to the scheme specified by the learning rule. This process was repeated while the prediction error decreased. After 1,000 learning epochs, the target was achieved and the learning stage was completed. In order to test the trained network, another data-set was used, and the input test set was presented to the network and the output was obtained. The output of the ANN was compared with the experimental data for the test data-sets in Table 1.

The coefficient of determination (R^2) and the mean square error (MSE) were used to test the statistical success of the models as shown in the following equations [27]:

$$R^2 = 1 - \frac{\sum_1^n (p_i - t_i)^2}{\sum_1^n (t_i - \bar{t})^2} \tag{11}$$

$$\mathrm{MSE} = \frac{1}{N}\sum_{K=1}^{N} (p_i - t_i)^2 \tag{12}$$

where p_i is the predicted, t_i is the target value, and $\bar{t}$ is the mean of the target values; and n is the total number of experiments.

MSE value for each network was calculated (as in Fig. 3). Considering the amount of MSE, the best network is (5-14-1). Addition to MSE, it is clear that the regression coefficient of determination is high between estimated and experimental response for this network (Figs. 4 and 5).

The relative importance of input variables on the value of AB 113 removal efficiency (%) obtained through the neural weight matrix is represented in Table 2 [28]. As can be seen, all of the independent variables strongly influence the AB 113 removal efficiency, but the effect of GOx activity is higher than of the other variables.

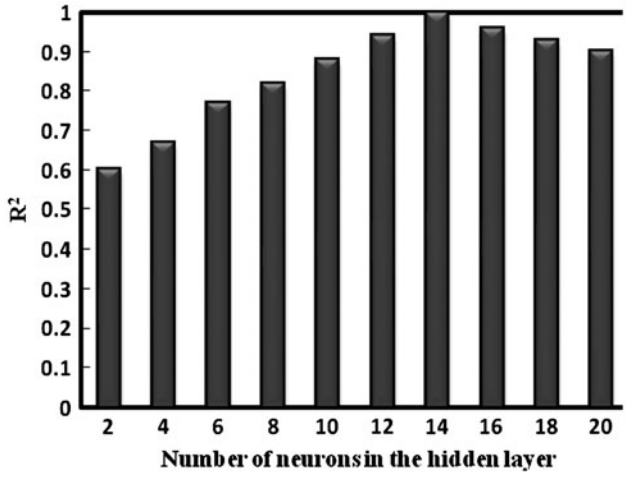

Fig. 4. Effect of the number of neurons in the hidden layer on the performance of the neural network (R^2).

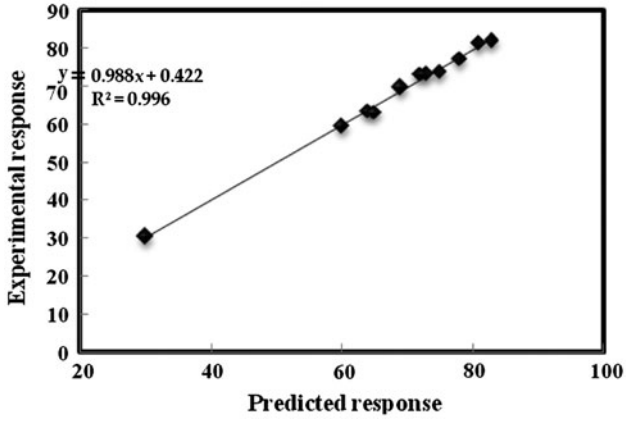

Fig. 5. Comparison of the experimental results with the calculated via neural network modeling for the test set.

Table 2
Relative importance of variables on decolorization efficiency of AB 113 which predicted by ANN

Variable	Importance (%)
Initial pH	23.35
Initial AB 113 concentration	19.5
Initial Fe^{2+} concentration	16.12
Initial glucose concentration	15.5
GOx activity	25.53
Total	100

4. Conclusion

This study demonstrates that Bio-Fenton reaction can decolorize a dye effluent without adding any external H_2O_2. This method, involving enzymatic *in situ* generation of H_2O_2, was developed for AB 113 decolorization. Effect of several parameters on Bio-Fenton process was investigated. The best conditions were achieved, and these are: Fe^{2+} concentration of 0.2 mmol/L, pH of 4.0, glucose concentration of 0.02 mol/L, and GOx activity of 3,000 U/L, at constant temperature (23 ± 0.1˚C) and shaking rate (160 rpm), while the concentration of AB 113 was 40 mg/L. In these conditions, AB 113 degradation efficiency after 60 min was resulted of ca 91%. Also, it was found that ANN with 5-14-1 structure with the best MSE (0.42×10^{-3}), and the coefficient of correlation (0.996). This proposed neural model can predict AB 113 removal from water by Bio-Fenton process.

References

[1] S. Jian-Hui, S. Shao-Hui, L. Yi-Fan, S. Sheng-Peng, Fenton oxidative decolorization of the azo dye Direct Blue 15 in aqueous solution, Chem. Eng. J. 98 (2009) 680–683.
[2] N. Daneshvar, D. Salari, A.R. Khataee, Photocatalytic degradation of azo dye Acid Red 14 in water: Investigation of the effect of operational parameters, J. Photochem. Photobiol. 157 (2003) 111–116.
[3] E. Chagas, L. Durrant, Decolorization of azo dyes by *Phanerochaete chrysosporium* and *Pleurotus sajorcaju*, Enzyme Microb. Technol. 29 (2001) 473–477.
[4] K. Umar, A.A. Dar, M.M. Haque, N.A. Mir, M. Muneer, Photocatalysed decolourization of two textile dye derivatives, Martius Yellow and Acid Blue 129, in UV-irradiated aqueous suspensions of titania, Desalin. Water Treat. 46 (2012) 205–214.
[5] İ.A. Şengil, A. Özdemir, Simultaneous decolorization of binary mixture of blue disperse and yellow basic dyes by electrocoagulation, Desalin. Water Treat. 46 (2012) 215–226.
[6] A.K. Yadav, L. Singh, A. Mohanty, S. Satya, T.R. Sreekrishnan, Removal of various pollutants from wastewater by electrocoagulation using iron and aluminium electrode, Desalin. Water Treat. 46 (2012) 352–358.
[7] K. Tanaka, K. Padarmpole, T. Hisanaga, Photocatalytic degradation of commercial azo dyes, Water Res. 34 (2000) 327–333.
[8] M. Muruganandham, N. Sobana, M. Swaminathan, Solar assisted photocatalytic and photochemical degradation of Reactive Black 5, J. Hazard. Mater. 137 (2006) 1371–1376.
[9] P. Mehta, R. Mehta, M. Surana, B.V. Kabra, Influence of operational parameters on degradation of commercial textile azo dye Acid Blue 113(Cyanine 5R) by advanced oxidation technology, J. Curr. Chem. Pharm. Sci. 1 (2011) 28–36.
[10] N. Chahbane, D. Popescu, D.A. Mitchell, A. Chanda, D. Lenoir, A.D. Ryabov, K. Schramm, T. Collins, Fe III-TAML-catalyzed green oxidative degradation of the azo dye Orange II by H_2O_2 and organic peroxides: Products, toxicity, kinetics and mechanisms, Green Chem. 9 (2007) 49–57.
[11] C. Segura, C. Zaror, H.D. Mansilla, M.A. Mondaca, Imidacloprid oxidation by photo-Fenton reaction, J. Hazard. Mater. 150 (2008) 679–686.
[12] J.C. Crittenden, J. Liu, D.W. Hand, D.L. Perram, Photocatalytic oxidation of chlorinated hydrocarbons in water, Water Res. 31 (2003) 429–438.
[13] M.M. Rahman, M.A. Hasnat, K. Sawada, Degradation of commercial textile dye by Fenton's reagent under xenon beam irradiation in aqueous medium, J. Sci. Res. 1 (2009) 108–120.
[14] N.K. Daud, U.G. Akpan, B.H. Hameed, Decolorization of Sunzol Black DN conc. in aqueous solution by Fenton oxidation process: Effect of system parameters and kinetic study, Desalin. Water Treat. 37 (2012) 1–7.

[15] J.A. Zazo, J.A. Casas, A.F. Mohedano, M.A. Gilarranz, J.J. Rodríguez, On the chemical pathway and kinetics of phenol oxidation by Fenton's reagent, Environ. Sci. Technol. 39 (2005) 9295–9302.
[16] I. Arsalan, I.A. Balcioglu, D.W. Babnemann, Advanced chemical oxidation of reactive dyes in simulated dyehouse effluents by ferrioxalate-Fenton/UV-A and TiO_2/UV-A processes, Dyes Pigm. 47 (2000) 207–218.
[17] A. Karimi, F. Mahdizadeh, M.R. Eskandarian, Enzymatic in-situ generation of H_2O_2 for decolorization of Acid Blue 113 by Fenton process, Chem. Ind. Chem. Eng. Q. 18 (2012) 89–94.
[18] D. Schäfer, M. Maciejewska, W. Schuhmann, SECM visualization of spatial variability of enzyme-polymer spots. 1. Discretisation and interference elimination using artificial neural networks, Biosens. Bioelectron. 22 (2007) 1887–1895.
[19] S.B. Bankar, M.V. Bule, R.S. Singhal, L. Ananthanarayan, Glucose oxidase—An overview, Biotechnol. Adv. 27 (2009) 489–501.
[20] M. Surana, P. Mehta, R. Mehta, B.V. Kabra, Photocatalytic degradation of commercial textile dye Acid Blue 113 by Photo-Fenton reagent in aqueous medium, J. Ind. Counc. Chem. 27 (2010) 190–193.
[21] A. Rathinam, N.F. Nishtar, R.R. Jonnalagadda, U.N. Balachandran, Wet oxidation of acid brown dye by hydrogen peroxide using heterogeneous catalyst Mn–salen–Y zeolite: A potential catalyst, J. Hazard. Mater. 138 (2006) 152–159.
[22] C. López, M.T. Moreira, G. Feijoo, J.M. Lema, Dye decolorization by manganese peroxidase in an enzymatic membrane bioreactor, Biotechnol. Progr. 20 (2004) 74–81.
[23] W. Aehle, Enzymes in industry: Production and applications, 2nd ed., Wiley-VCH, New York, pp. 527–530, 2007.
[24] X.R. Xu, Z.Y. Zhao, X.Y. Li, J.D. Gu, Chemical oxidative degradation of methyl tert-butyl ether in aqueous solution by Fenton's reagent, Chemosphere 55 (2004) 73–79.
[25] M. Chang, J.M. Chern, Decolorization of peach red azo dye, HF_6 by Fenton reaction: Initial rate analysis, J. Taiwan Inst. Chem. Eng. 41 (2010) 221–228.
[26] K. Huang, F. Chen, D. Lü, Artificial neural network-aided design of a multi-component catalyst for methane oxidative coupling, Appl. Catal. A 219 (2001) 61–68.
[27] M. ErdemGünay, I. EmrahNikerel, E. ToksoyOner, B. Kirdar, R. Yildirim, Simultaneous modeling of enzyme production and biomass growth in recombinant *Escherichia coli* using artificial neural networks, Biochem. Eng. J. 42 (2008) 329–335.
[28] M. Zarei, A.R. Khataee, R. Ordikhani-Seyedlar, M. Fathinia, Photoelectro-Fenton combined with photocatalytic process for degradation of an azo dye using supported TiO_2 nanoparticles and carbon nanotube cathode: Neural network modeling, Electrochim. Acta 55 (2010) 7259–7265.